Science and Technology for Energy Transition **79**, 30 (2024)

https://doi.org/10.2516/stet/2024026

Available online at:
stet-review.org

**Decarbonizing Energy Systems: Smart Grid and Renewable Technologies**
Fang Rui-ming and Qiangqiang Liao (Guest Editors)

REGULAR ARTICLE OPEN ACCESS

# A method to design contact-separation triboelectric nanogenerators (CS-TENG) for efficient vibration energy harvesting

Meriam Khelifa* and Audrey Iranzo

Capgemini Engineering, Direction Recherche and Innovation, 4 Avenue Didier Daurat, 31700 Blagnac, France

Received: 13 September 2023 / Accepted: 8 April 2024

**Abstract.** The necessity of self-powered electronic devices for sensing and communication (IoT) has led to the development of methods for energy harvesting. Triboelectric Nanogenerators (TENG) are promising for harvesting mechanical energy from the environment, in particular energy from vibrations. The optimization of the efficiency of energy transfer from vibration energy into electrical energy is a crucial problem. This paper deals with a contact-separation TENG (CS-TENG) devoted to vibration harvesting. Optimization was carried out taking into account all the parameters of the TENG connected to a load resistance. The moving electrode of the CS-TENG was supposed to be sinusoidal. After transformation into dimensionless parameters and variables intervening in the problem, it appeared that the electrical dynamics of the TENG are intrinsically determined by only two dimensionless parameters. Consequently, the optimization of efficiency can be conducted in a two-dimensional space. It is shown that the maximum efficiency of a TENG permanently connected to the load resistance cannot be greater than 25%. However, the efficiency can be increased to nearly 100%, provided that a switch is used in series with the load resistance which opens and closes in synchronization with the electrode motion. The optimization method presented could be extended to design TENG energy harvesters operating in other modes and for arbitrary vibrations.

**Keywords:** Vibrations harvesting, Triboelectric nanogenerators, TENG efficiency.

## 1 Introduction

Harvesting all the available sources of energy in the environment (mechanical, thermal, electromagnetic) has become a fundamental issue with the multiplication of connected objects in the environment, such as sensor networks, which makes the development of self-powered electronic devices for wireless communication [1, 2]. Thermal energy is abundant, but its conversion to electrical energy is limited by the Carnot efficiency [3]. Harvesting mechanical energy from the environment to produce electrical energy is more promising, as the conversion efficiency can in principle reach 100%, which is a determinant advantage to power low-power systems. Moreover, the constraint of developing environmentally friendly devices focused research since 2012 on the development of triboelectric generators to convert mechanical to electrical energy [4, 5]. The principal advantage of triboelectric nanogenerators, commonly named TENGs, is that they can be fabricated from low cost environmentally friendly materials. The fabrication of TENGs requires thin layers of materials, which facilitates the fabrication and reduces the cost.

So far, many applications of TENGs already emerged, such as medical applications [6, 7]. Also, TENGs were developed for harvesting the energy of wind and ocean waves [8, 9]. The hybridization of a TENG with a piezoelectric generator was also explored [10].

Basically, a contact-separation (CS) TENG is represented by Figure 1. The generator consists of a capacitor whose upper electrode is mobile and the lower electrode is fixed and grounded. A dielectric layer of thickness $h_d$ and relative permittivity $\varepsilon_r$ is attached to the lower electrode. The CS-TENG is also characterized by the triboelectric charge density $\sigma$ distributed on an area $A_d$. Due to the numerous parameters to optimize, a profound understanding of the conversion mechanism of a TENG is required in order to achieve optimal performance. If a TENG is devoted to harvesting energy, it seems relevant to focus the study on the maximization of energy output. In this context, Zi *et al.* [11] defined a figure-of-merit (FOM) for a TENG, which has the advantage of allowing the comparison of performance of TENGs operating with different modes. Also, the additional advantage of FOM is to

* Corresponding author: meriam.khelifa@capgemini.com

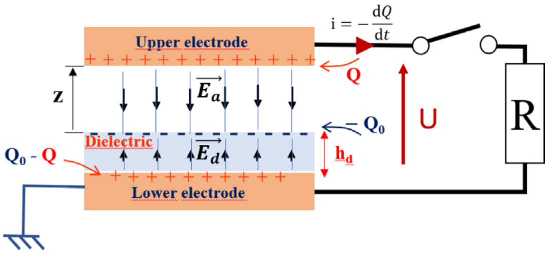


**Fig. 1.** Diagram of a contact-separation (CS) triboelectric nanogenerators.

characterize the TENG performance independently of the triboelectric charge density, $\sigma$. However, the performance of a triboelectric generator may be characterized by different criteria, depending on the intended application of the TENG. Vasandani *et al.* [12] focused on the maximization of the output voltage of a CS-TENG. Using the design of experiment (DOE) methodology, the authors of [12] studied the effect of three parameters (the device area $A_\mathrm{d}$, the maximum vibration displacement $z_\mathrm{max}$ and the dielectric thickness $h_\mathrm{d}$), while the TENG was in an open circuit. Adly *et al.* [13] chose to maximize the voltage per volume $V_\mathrm{d}$ of the device ($V_\mathrm{d} = A_\mathrm{d} \times z_\mathrm{max}$) by varying the resistance $R$ and the dielectric thickness $h_\mathrm{d}$, using the design of experiment methodology. Zi *et al.* [11] presented results which demonstrate the existence of an optimum displacement $z_\mathrm{max}$ of the electrode which maximizes efficiency.

Many studies highlighted the importance of the description of the cyclic operation of a TENG by a voltage-charge diagram (U-Q diagram) for the evaluation of the energy transferred to the load resistance [14–17]. Meng and Chen [17] pointed out that the conversion efficiency of a TENG could reach 100%, provided that a switch is used during the triboelectric cycle. If the resistive load $R$ is disconnected from the TENG during the upward movement of the electrode, electrostatic energy is stocked within the electric field. Then, this electrostatic energy can be released into the load before the electrode goes back in contact with the dielectric.

The actual efficiency of the TENG depends on many parameters (at least four parameters are required to characterize a CS-TENG). In addition, the vibration characteristics (frequency, amplitude) are parameters to be considered for optimization of efficiency. It seems difficult to take account of all the parameters in an optimization process. This paper attempts to take into account all the parameters in the optimization process. The theoretical study that is presented concerns the optimization of a CS-TENG.

The paper first presents the theory of a CS-TENG, where it is shown that all the parameters of a TENG can be reduced to only two dimensionless parameters named $\alpha$ and $\beta$. In Section 2, the determination of optimum parameters $\alpha$ and $\beta$ is conducted for two different situations: (i) the TENG is permanently connected to a load resistance $R$, and (ii) a switch is used to connect or disconnect the load $R$ during the triboelectric cycle. Section 3 illustrates how the results of the preceding section can be used to design an optimized TENG, once the size of the device, frequency and amplitude of the vibrations are specified.

## 2 Theory

### 2.1 Triboelectric cycle

Triboelectric generators are energy converters that can potentially convert 100% of mechanical energy into electrical energy. The triboelectric charges are assumed to be uniformly distributed over the upper surface of the dielectric with density $-\sigma$ (assume that triboelectric charges are negative). The total triboelectric charge is $-Q_0 = -\sigma A_\mathrm{d}$, where $A_\mathrm{d}$ is the area of the capacitor. The density of triboelectric charge $-\sigma$ is assumed constant during operation. It will be shown in this section that if this assumption is not fulfilled, the results of the study are not changed.

The harvesting of vibrations is based on the oscillation of the upper electrode which periodically comes in contact with the dielectric. The device has a cyclic operation, which is depicted in Figure 2a. The cycle has four steps described as follows:

1. In the initial state of the generator, the mobile electrode is in contact with the dielectric ($z = 0$) and the capacitor is in short-circuit. The upper electrode carries a total positive charge $Q_0$ which neutralizes the triboelectric charge $-Q_0$. The lower electrode has no charge so the capacitor voltage $U$ is zero. Due to the two opposite charges, an attractive electrostatic force $F_\mathrm{e} = \frac{\sigma^2}{2\epsilon_0} \times A_\mathrm{d}$ exists between the upper electrode and the dielectric. From this state, the mobile electrode will have an upward movement during which the charges remain constant. To do so, the capacitor is in an open circuit during the displacement of the electrode.

2. In this state, the mobile electrode has reached the position $z = z_\mathrm{max}$. During the displacement from $z = 0$ to $z = z_\mathrm{max}$, the electrostatic force is counterbalanced by an external force which does mechanical work. This results in an increase in the electrostatic potential energy of the capacitor. The electrostatic energy increases linearly with the displacement $z$ of the electrode. In this state, the capacitor has stored electrostatic energy:

$$\mathcal{E}_\mathrm{e}^\mathrm{max} = \frac{\sigma^2}{2\epsilon_0} \times A_\mathrm{d} \times z_\mathrm{max} \tag{1}$$

3. In this state, the position of the mobile electrode is still $z = z_\mathrm{max}$. Before the electrode starts to return, the charge of the mobile electrode is cancelled, by driving the charge $Q_0$ from the upper electrode to the lower electrode, using an external circuit. The voltage goes from $U_\mathrm{max} = \frac{\sigma}{\varepsilon_0} \times z_\mathrm{max}$ to $U_\mathrm{min} = -\frac{\sigma}{\varepsilon_0 \varepsilon_r} \times h_\mathrm{d}$ during the charge transfer. Note that the external circuit cannot be a simple resistance but an active circuit.

4. In this state, the position of the mobile electrode is again $z = 0$. During the backward movement, the charge was maintained to zero, so that no work could be done by the external force during the step from $z = z_\mathrm{max}$ to $z = 0$. In order to recover the initial state, the charge $Q_0$ has to be driven back from the lower electrode to the upper electrode.

Now, a balance sheet of the energy transferred to the external circuit during the triboelectric cycle previously

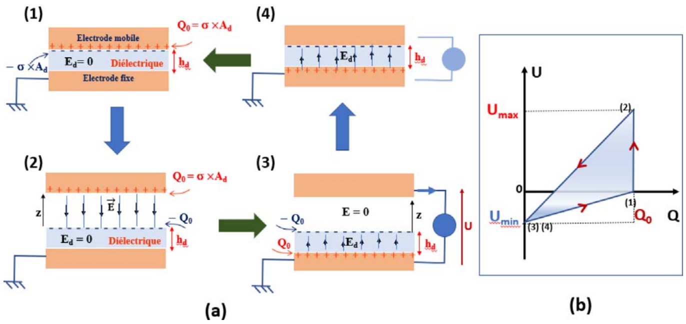


**Fig. 2.** Triboelectric cycle: a) steps of ideal triboelectric cycle, b) voltage-charge diagram of the cycle.

described is drawn. Figure 2b represents the cycle in a voltage-charge diagram (U-Q diagram). The electrical energy transferred to the load $R$ during a cycle is:

$$E_{\text{cycle}} = -\oint U\mathrm{d}Q. \tag{2}$$

The transferred energy, represented by the area of the cycle in Figure 2b is:

$$E_{\text{ref}} = \frac{1}{2}U_{\max}Q_0. \tag{3}$$

This output energy $E_{\text{ref}}$ is taken as the reference output energy, as it is the maximum energy that can be transferred per cycle. If the external circuit does not have the ideal behavior, for example, a resistance $R$ permanently connected, it will be shown that the output energy $E_{\text{cycle}}$ is inferior to $E_{\text{ref}}$. So the efficiency of energy transfer to the external harvester circuit is defined by:

$$\eta = \frac{E_{\text{cycle}}}{E_{\text{ref}}}. \tag{4}$$

Note that the above definition of the efficiency coincide with the figure-of-merit (FOM) defined by Zi *et al.* [11], which is:

$$\text{FOM} = \frac{2\epsilon_0}{\sigma^2}\frac{E_{\text{cycle}}}{A_{\text{d}}z_{\max}}. \tag{5}$$

Indeed, $E_{\text{ref}} = \frac{1}{2}U_{\max}Q_0 = \frac{1}{2}\frac{\sigma}{\varepsilon_0}z_{\max}\sigma A_{\text{d}}$. Substitution of the last expression in equation (4) leads to equation (5). Note that the reference energy defined by Meng and Chen [17] is slightly different than in equation (3), as the authors consider a different reference cycle, where negative external work is done during the backward translation of the mobile electrode and they considered that this work has to be removed from the balance sheet.

## 2.2 Dynamics equation of the CS-mode triboelectric generator

In Figure 1, a switch is present in the circuit. Firstly, considering that the switch remains permanently closed, the resistance $R$ is continuously connected to the TENG. Section 3.2 deals with the case where the switch is closed and opened intermittently depending on certain switching levels.

### *2.2.1 Differential equation for the charge Q*

In Appendix A, it is shown that the charge $Q$ carried by the mobile electrode evolves according to the following differential equation of first order:

$$R\frac{\mathrm{d}Q}{\mathrm{d}t} = \frac{\sigma h_{\text{d}}}{\varepsilon_0\varepsilon_r} - \frac{1}{A_{\text{d}}\varepsilon_0}\left(z + \frac{h_{\text{d}}}{\varepsilon_r}\right)Q. \tag{6}$$

The motion of the electrode is assumed to be described by a periodic function $z(t)$. The solution $Q(t)$ of equation (6) is the sum of a transient solution and a steady-state solution. The analysis of the energy exchange between the generator and the load $R$ can be done using the $U$-$Q$ diagram [11, 17]. The voltage $U$ across $R$ and the current $I = -\mathrm{d}Q/\mathrm{d}t$ in the receiver convention for the load $R$ gives an instantaneous power dissipation $P(t) = -U\,\mathrm{d}Q/\mathrm{d}t$. The energy dissipated in the load $R$ over a cycle, during a steady state regime is given by equation (2) so that the efficiency $\eta$ of the energy transfer from mechanical to electrical is equation (4). The problem is to find the set of parameters of the CS-TENG which provides the maximum efficiency $\eta$. First of all, it is mandatory to identify the parameters that intrinsically govern the electrical dynamics of the charge $Q$ in equation (6). It can be seen that equation (6) is *a priori* determined by four parameters: $\sigma$, $A_{\text{d}}$, $h_{\text{d}}/\varepsilon_{\text{r}}$ (effective dielectric thickness) and $R$. Moreover, the motion $z(t)$ of the mobile electrode in equation (6) must be specified. This motion is assumed to be sinusoidal: $z(t) = \frac{z_{\max}}{2}(1 + \sin 2\pi ft)$, where $z_{\max}$ is the peak-to-peak amplitude and $f$ is the vibration frequency.

The problem to solve is the following: once the motion of the electrode, *i.e.* $z_{\max}$ and $f$ fixed, find the parameters of the TENG which provides the maximum efficiency $\eta$. To solve this problem, it is useful to transform equation (6) into dimensionless form. The advantage of this transformation is to reveal which parameters intrinsically determine efficiency $\eta$.

### *2.2.2 Dimensionless dynamical equation*

Firstly, the dimensionless time is obtained by dividing the real time $t$ by the vibration period $T = 1/f$. Secondly, the dimensionless coordinate is obtained by dividing the real coordinate $z$ by the peak-to-peak amplitude $z_{\max}$. In the following, the symbols $t$ and $z$ will represent the dimensionless time and coordinate. Then, the dimensionless displacement of the electrode is written:

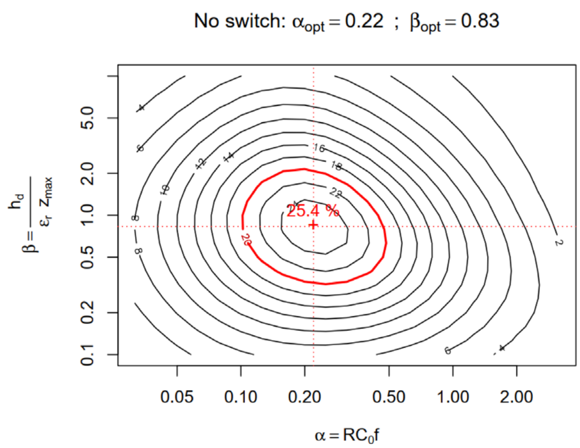


**Fig. 3.** Resistance permanently connected to the TENG. Contour plot of efficiency $\eta$ versus parameters $\alpha$ and $\beta$.

$$z(t) = \frac{1}{2}(1 + \sin 2\pi t). \tag{7}$$

The electric charge $Q$ and the voltage $U$ have to be replaced by the dimensionless charge $q = Q/Q_0$ and voltage $u = U/U_{\max}$, where the charge reference $Q_0 = \sigma A_d$ is the total triboelectric charge, which is assumed constant. The voltage is normalized to the maximum voltage $U_{\max} = \frac{\sigma}{\varepsilon_0} \times z_{\max}$. Using equations (2) and (3), the efficiency can be rewritten in terms of the dimensionless variables $u$ and $q$:

$$\eta = -2 \oint u \, \mathrm{d}q. \tag{8}$$

In the Appendix A, it is shown that the dimensionless voltage is: $u = qz - \beta(1 - q)$, where $\beta = h_d/(\varepsilon_r\ z_{\max})$ is the ratio of effective dielectric thickness to the peak-to-peak amplitude of vibrations. Taking account that the integration of $\beta(1 - q)$ over a cycle is zero, as it must be for a state function, the expression of $\eta$ is simplified as follows:

$$\eta = -2 \oint qz \, \mathrm{d}q. \tag{9}$$

Equation (9) shows that the efficiency of a CS-TENG is only determined by the evolution of the dimensionless charge $q$ and coordinate $z$. In Appendix A, it is shown that the differential equation for the variable $q$ is:

$$\frac{\mathrm{d}q}{\mathrm{d}t} = \frac{1}{\alpha}\left[1 - \left(1 + \frac{z}{\beta}\right)q\right]. \tag{10}$$

The first dimensionless parameter of equation (10) is $\alpha = R/R_0$, which is defined as the normalized resistance with the reference resistance $R_0 = T/C_0$, where $C_0 = \varepsilon_0\varepsilon_r A_d/h_d$ is the reference capacitance of the TENG. The capacitance $C_0$ is the capacitance of the TENG when the mobile electrode is in contact with the dielectric, *i.e.* $z = 0$. If the resistance $R$ is permanently connected to the TENG (switch permanently closed), equation (10) shows that the evolution of $q(t)$ is only determined by the two dimensionless parameters $\alpha$ and $\beta$. Consequently the efficiency $\eta$ only depends on these two parameters. Equation

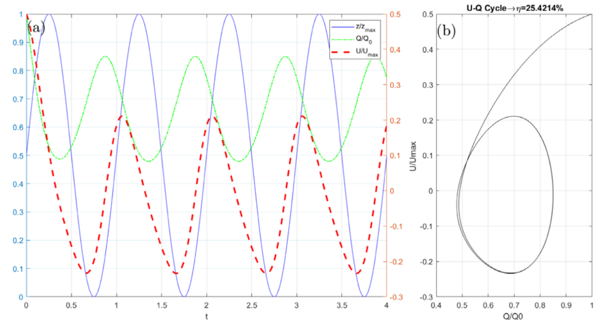


**Fig. 4.** Optimal solution of equation (10) without switching. The optimum parameters are: $\alpha_{opt} = 0.22$ and $\beta_{opt} = 0.83$. a) Left vertical axis: dimensionless motion of the electrode $z(t)$ (blue solid line) and charge $q(t)$ (green dot-dash line). Right vertical axis: voltage $u(t)$ (thick red dashed line). b) U-Q cycle in dimensionless variables, showing efficiency of 25.4%, calculated in the steady state regime.

(10) shows that the evolution of the dimensionless charge $q(t)$ does not depend on the triboelectric charge density $\sigma$. So, the search for the maximum of the function $\eta(\alpha, \beta)$ has to be performed in a two-dimensional space (2D). The search of optimum parameters $\alpha_{opt}$ and $\beta_{opt}$ which lead to the maximum of $\eta$ will be studied in Section 3.1. In the case where the switch is opened and closed in synchronization with the electrode motion, at least one additional parameter $S_L$ (switching level) must be used to specify when the switch must open and close. Then, the optimum parameters $\alpha_{opt}$ and $\beta_{opt}$ are functions of parameter $S_L$. This situation will be discussed in Section 3.2. Once the optimum values $\alpha_{opt}$ and $\beta_{opt}$ are found, it is easy to go back to the real parameters $h_d$ and $R$ of the TENG.

### *2.2.3 Calculation of efficiency η*

The numerical resolution of equation (10) can be performed with the *xcos* module of Scilab, an alternative to the *Simulink* module of Matlab. Once the two parameters $\alpha$ and $\beta$ are chosen, equation (10) is solved to find the evolution of the dimensionless charge $q(t)$ with initial charge $q(t = 0) = 1$. The solution $q(t)$ displays a transient regime whose duration is of the order of the time constant $RC_0$. The parameter $\alpha = \frac{RC_0}{T}$, can be considered as the normalized time constant, so the calculation must be performed until the system reaches the steady state regime of the TENG ($t \geq 2\alpha$), which requires several periods of vibration if $\alpha < 1$ (see Figs. 4 and 5). The efficiency $\eta$ is calculated using equation (9) over one period in the steady state regime.

## 3 Optimization

Due to the numerous parameters governing the functioning of a TENG (see Table 1), optimization of TENG efficiency would be *a priori* a hard task. Fortunately, the normalization of variables and parameters has led to a drastic simplification of the problem to be solved. Now, the problem is reduced to the search of only two optimum parameters $\alpha_{opt}$ and $\beta_{opt}$.

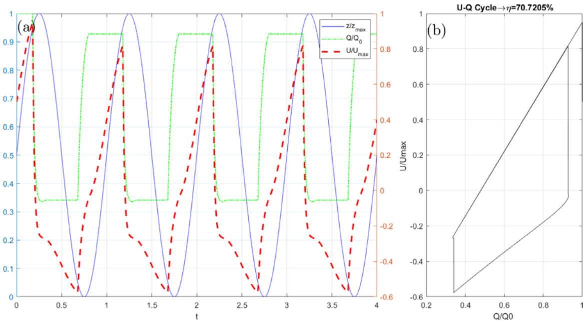


**Fig. 5.** Solution of equation (10) at switching levels $S_L = 0.05$ and $S_H = 0.95$, for dimensionless parameters $\alpha = 0.05$ and $\beta = 0.5$. This solution is not optimal for the switching level $S_L = 0.05$. a) Left vertical axis: dimensionless motion of the electrode $z(t)$ (blue solid line) and charge $q(t)$ (green dotdash line). Right vertical axis: voltage $u(t)$ (red dashed line). b) U-Q cycle in dimensionless variables, showing efficiency of 70.7%.

In this section, the situation where the TENG is always connected to the load resistance resistance $R$ is first considered (switch permanently closed). Then, the case of a switch that is opened and closed in synchronization with the motion of the electrode is studied.

## 3.1 Resistance permanently connected to the generator

The resistance $R$ is always connected during the cycle. The problem is to search the parameters $\alpha_{opt}$ and $\beta_{opt}$ which give the maximum efficiency $\eta$ defined by equation (9). In this case, efficiency $\eta$ is calculated on a grid of values of $\alpha$ and $\beta$ in order to plot the contour map of Figure 3. The plot clearly shows that there is only one maximum of efficiency at the point $\alpha_{opt} = 0.22$ and $\beta_{opt} = 0.83$, which gives the maximum efficiency $\eta_{max} = 25.4\%$. The contour line at 20% shows that efficiency $\eta$ is not very sensitive to variations of parameters $\alpha$ and $\beta$. Indeed, if $0.1 < \alpha < 0.5$ and $0.25 < \beta < 2$ then $\eta > 20\%$. For example, if the TENG is designed optimally for a given vibration frequency, then if the frequency has been doubled or halved ($\alpha$ doubled or halved), the efficiency does not fall abruptly, so the TENG remains close to the maximum efficiency. Also, if the amplitude of vibrations has been doubled or halved ($\beta$ halved or doubled), the efficiency of the TENG remains close to its maximum.

At the optimum point, the evolution of the reduced voltage $u(t)$ and charge $q(t)$ as a function of the time is shown in Figure 4a. The corresponding $U$-$Q$ cycle is shown in Figure 4b. One can observe that during the forward motion, the charge $Q$ is at its highest level, whereas during the backward motion, the charge $Q$ is at its lowest level. This remark gives a hint on what must be done to improve efficiency. The charge $Q$ must be as large as possible during the upward movement of the electrode, whereas $Q$ must be as close to zero as possible during the downward movement.

Unfortunately, with the switch permanently closed, efficiency is capped at about 25%. In order to improve TENG efficiency, it is mandatory to use a switch which closes and opens in synchronization with the motion of the electrode.

**Table 1.** Definition of basic parameters of the TENG.

| Parameters | Label |
|---|---|
| TENG area | $A_d$ |
| Dielectric thickness | $h_d$ |
| Dielectric constant | $\varepsilon_r$ |
| Vacuum permittivity | $\varepsilon_0$ |
| TENG capacitance at zero gap | $C_0$ |
| Triboelectric charge density | $\sigma$ |
| Vertical position of the moving electrode | $z(t)$ |
| Vibration frequency | $f$ |
| Peak-to-peak vibration amplitude | $z_{max}$ |
| Voltage at TENG terminals | $U$ |
| Electrical charge carried by the mobile electrode | $Q$ |
| Load resistance | $R$ |
| Output energy transferred to the load $R$ during a TENG cycle | $E_{cycle}$ |
| Maximum output energy during a TENG cycle | $E_{ref}$ |
| Energy efficiency | $\eta = \frac{E_{cycle}}{E_{ref}}$ |
| Lower switching level | $S_L$ |
| Higher switching level | $S_H$ |
| Normalized load resistance | $\alpha = RC_0 f$ |
| Normalized dielectric thickness | $\beta = \dfrac{h_d}{\varepsilon_0\, z_{max}}$ |

## 3.2 Synchronized switching

The switch is opened and closed at particular positions $z(t)$ of the electrode (in dimensionless variable $0 \le z \le 1$). A lower switching level $S_L$ is defined. The switch is closed if $z(t) \le S_L$ or $z(t) \ge S_H$, else the switch is open. When the switch is open the electric current is zero. So, equation (10) becomes $\frac{dq}{dt} = 0$, *i.e.* $q$ is constant.

For the sake of simplification, a single parameter is chosen for the switching. The lower switching level, $S_L$ determines the higher switching level, which is $S_H = 1 - S_L$. As the switching level $S_L$ gets closer and closer to 0, $S_H$ gets closer and closer to 1.

To illustrate the effect of switching on efficiency, a calculation was performed with switching levels $S_L = 0.05$ and $S_H = 0.95$, and parameters $\alpha = 0.05$ and $\beta = 0.5$, which are not the optimum parameters. The calculated efficiency is 70.7%, which is a considerable gain compared to no switching (see Fig. 5). It is reasonable to think that a switching level $S_L$ close to zero would increase efficiency, but the closing and opening of the switch at very close times, require a very short switching time and a fast transfer of the electric charge.

A more systematic study was conducted by varying the switching level $S_L$ in the range of [0.2%; 50%]. Note the switching level of 50% means that the switch remains closed all the time, so the load is permanently connected to the TENG. The search of optimum parameters $\alpha_{opt}$ and $\beta_{opt}$

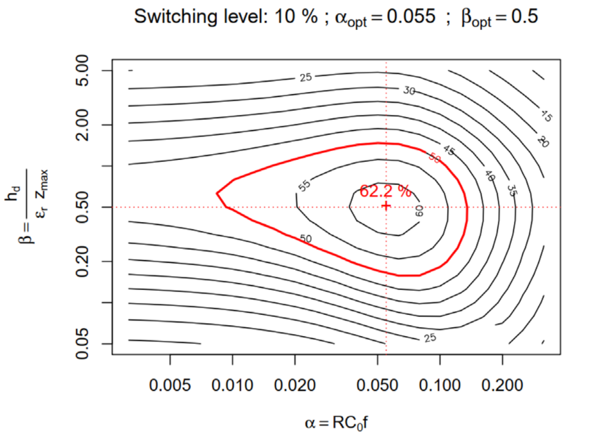


**Fig. 6.** Resistance permanently connected to the TENG. Contour plot of efficiency $\eta$ versus parameters $\alpha$ and $\beta$.

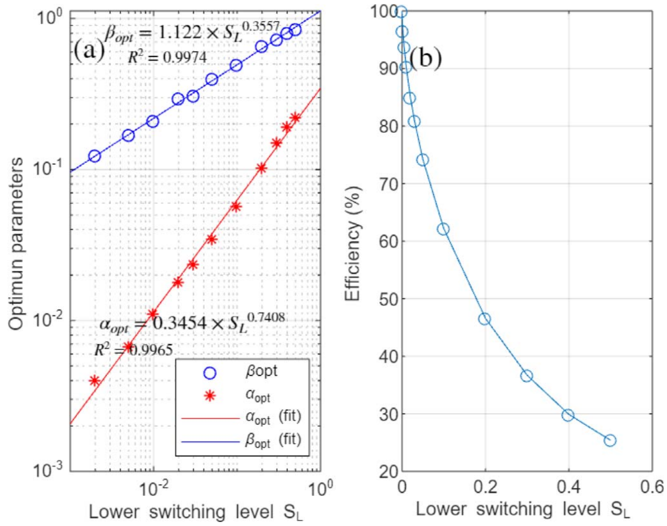


**Fig. 7.** a) Evolution of the optimum parameters $\alpha_{opt}$ and $\beta_{opt}$ as a function of the lower switching level $S_L$. The relationships between optimum parameters and $S_L$ are obtained from the linear fit of the data in the log-log plot. b) Evolution of the optimum efficiency $\eta_{opt}$ as a function of the lower switching level $S_L$.

was conducted by a systematic exploration of a domain of variation of $\alpha$ and $\beta$ in order to plot a contour map of the function $\eta(\alpha, \beta)$, for a fixed value of the switching level $S_L$ (see the example of Fig. 6 for $S_L = 10\%$). Figure 7a shows the evolution of optimum parameters $\alpha_{opt}$ and $\beta_{opt}$ as a function of $S_L$ and Figure 7b shows the evolution of efficiency $\eta_{opt}$ as a function of the switching level $S_L$. Figure 7a shows the linear fit of the data with $S_L$ in a log-log plot. So the evolution of the optimum parameters can be approximated by the following functions:

$$\alpha_{opt} = 0.3454 \times {S_L}^{0.7408} \tag{11}$$

and

$$\beta_{opt} = 1.122 \times {S_L}^{0.3557}. \tag{12}$$

A similar approximate expression can be written for the optimum efficiency:

$$\eta_{opt} = 100 \times \left(1 - 1.600 \times {S_L}^{0.6073}\right). \tag{13}$$

Equation (13) is valid only if $S_L \leq 0.05$. For $S_L$ between 0.05 and 0.5, a polynomial fit is suitable to model $\eta_{opt}$ versus $S_L$.

For each value of switching level $S_L$, the contour map displays a single maximum. For example, the contour map of Figure 6 shows the maximum of efficiency for the switching level $S_L = 10\%$ at the point of coordinates: $\alpha_{opt} = 0.055$ and $\beta_{opt} = 0.5$, with a maximum $\eta_{opt} = 62.2\%$. It is remarkable that, about the optimum point, efficiency is not sensitive to any change in parameters $\alpha$ and $\beta$. The contour line at 50% efficiency shows the domain where $\eta \geq 50\%$. Thus, a TENG designed at the optimum point remains efficient even if the frequency and amplitude have been doubled or halved.

The practical uses of equations (11) and (12) will be presented in the Section 4.

## 4 Case studies

In this section, we present the application of the results presented in Section 3. Any dimensionless set of parameters $\alpha$, $\beta$, and $S_L$ corresponds to a class of TENGs in the real world, *i.e.* many generators (in theory an infinity) with very different parameters, *i.e.* with different parameters: $A_d$, $h_d$, and different vibration frequencies $f$ and amplitudes $z_{max}$, may correspond to the same set of values $\alpha$ and $\beta$. The design of three optimized TENG will illustrate the use of dimensionless parameters $\alpha$ and $\beta$, each TENG belonging to a different class.

The three generators, each harvesting vibrations of different amplitudes $z_{max}$ and frequencies $f$, have different sizes $A_d$. For the three generators, the same insulating material was chosen, with the dielectric constant $\varepsilon_r = 3.4$, and the identical triboelectric charge density $\sigma = 10\ \mu\mathrm{Cm}^{-2}$. As highlighted previously, triboelectric charge density $\sigma$ has no influence on efficiency, but it determines the electrical power delivered by the generator, which is proportional to $\sigma^2$. Note that $\sigma$ also determines the electric field in the air gap, which is $E_a = \frac{\sigma}{\varepsilon_0} = 1.13\ MV\ \mathrm{m}^{-1}$. This value of $E_a$ is below the breakdown electric field of 3 MV $\mathrm{m}^{-1}$ [18]. Once the frequency $f$ and the amplitude $z_{max}$ are defined, the optimum dielectric thickness and the optimum load resistance are readily calculated as follows:

$$(h_d)_{opt} = \beta_{opt} \times \varepsilon_r z_{max} \tag{14}$$

and

$$R_{opt} = \alpha_{opt} \times T \times \frac{(h_d)_{opt}}{\varepsilon_0 \varepsilon_r A_d}. \tag{15}$$

Note that the optimum dielectric thickness is not explicitly frequency-dependent.

In these examples, the vibration amplitudes $z_{max}$ are chosen by imposing the same acceleration $a_{max} = 50\mathrm{g} \approx 500$. So, the peak-to-peak amplitude is: $z_{max} = \dfrac{2 \times a_{max}}{(2\pi f)^2}$.

**Table 2.** Characteristics of the three designed triboelectric generators.

| Generators characteristics | Generator #1 | Generator #2 | Generator #3 |
|---|---|---|---|
| Lower switching level: $S_L$ | 0.2% | 10% | 50% |
| Efficiency: $\eta$ (%) | 96.5 | 62.2 | 25.4 |
| Working frequency: $f$ (Hz) | 200 | 2000 | 5000 |
| Capacitor area: $A_d$ ($m^2$) | 0.1 | 0.01 | 0.001 |
| Peak-to-peak amplitude: $z_{max}$ (μm) | 633 | 6.33 | 1.01 |
| Maximum voltage: $U_{max}$ (V) | 716 | 7.16 | 1.15 |
| Dielectric thickness: $h_d$ (μm) | 265 | 10.7 | 3.0 |
| Optimum load resistance: $R_{opt}$ (Ohm) | 1524 | 1112 | 4155 |
| Output average power: $P_{av}$ (mW) | 6910 | 44.5 | 0.7 |

A minimum time delay between two successive switching $\Delta t_{min} = 100$ is chosen, which is not very fast but sufficient to take into account of the switching time and the time necessary to transfer the electrical charge from one electrode to the other. For each generator, the minimum possible switching level $S_L$ is calculated. Then, once the switching level $S_L$, the optimum parameters: $\alpha_{opt}$, $\beta_{opt}$ are readily determined using equations (11) and (12). Table 2 summarizes the characteristics of each designed TENG. The average power $P_{av}$ delivered by the generators is mentioned.

Generator #1:
The frequency of vibrations is 200 Hz. The choice of $S_L = 0.2\%$ is possible ($S_H = 99.8\%$), which provides efficiency $\eta = 96.5\%$.

Generator #2:
The frequency of vibrations is 2000 Hz. The choice of $S_L = 10\%$ is possible ($S_H = 90\%$), which provides efficiency $\eta = 62.2\%$.

Generator #3:
The frequency of vibrations is 5000 Hz. No switching is possible at this frequency with $\Delta t_{min} = 100$. The resistance is connected permanently, so efficiency $\eta = 25.4\%$.

The optimum values of the load resistance $R$ are all of the order of kΩ. It is worth pointing out that if the vibration frequency changes, there is the possibility of conserving $\alpha_{opt}$ if one changes the load resistance $R$ so that $\alpha_{opt}$ remains constant, and then efficiency can remain unchanged. From the results of Section 3, efficiency is not very sensitive to any change in vibration amplitude with a factor between 0.5 and 2.0.

## 5 Conclusion

A study of CS-TENGs devoted to vibration energy harvesting was presented. The study aims to provide a tool useful to easily design a CS-TENG with the highest efficiency. The design of a CS-TENG necessitates the specification of at least 4 parameters: the device area $A_d$, the dielectric thickness $h_d$, the load resistance $R$ and the triboelectric charge density $\sigma$. Additional parameters are necessary to specify the vibration frequency and amplitude. As far as the designer is only concerned with the efficiency, it was demonstrated that the intrinsic dynamics of a CS-TENG are only determined by two dimensionless parameters: i) $\alpha = RC_0 f$, which is the normalized load resistance and ii) $\beta = \frac{h_d}{\epsilon_0 z_{max}}$, which is the normalized dielectric thickness. In consequence, the optimization of the efficiency of a TENG is considerably simplified by the reduction of the number of parameters to optimize. The case of a sinusoidal motion of the electrode was studied, with frequency $f$ and peak-to-peak amplitude $z_{max}$. The first important result is that there is only one optimum solution $\alpha_{opt}$ and $\beta_{opt}$ which maximizes efficiency. The second important result is that to obtain the maximum efficiency (in principle 100% efficiency achievable), it is mandatory to use switching, which isolates the TENG from the load during the motion of the electrode, except in the vicinity of turning points. Without switching, efficiency would be limited to a value of about 25%. Another important result of the study is the following: in the vicinity of the optimum point, efficiency varies very slowly. An optimized TENG designed for a given frequency and amplitude of vibration is still efficient even if the frequency or the amplitude is doubled or halved. In other words, the efficiency of a TENG can be made practically independent of the conditions of vibration.

It would be interesting in future work to apply the method described in this paper to other modes of TENGs, such as the lateral sliding (LS) mode in order to satisfy the need for a new efficient mechanical energy harvester.

## References

1 Ahmed A., Hassan I., El-Kady M.F., Radhi A., Jeong C.K., Selvaganapathy P.R., Zu J., Ren S., Wang Q., Kaner R.B. (2019) Integrated triboelectric nanogenerators in the era of the Internet of things, *Adv. Sci.* **6**, 24, 1802230.
2 Li J., Wu C., Dharmasena I., Ni X., Wang Z., Shen H., Huang S.-L., Ding W. (2020) Triboelectric nanogenerators enabled internet of things: a survey, *Intell. Converg. Netw.* **1**, 2, 115–141.
3 Kumar P.M., Babu V.J., Subramanian A., Bandla A., Thakor N., Ramakrishna S., Wei H. (2019) The design of a thermoelectric generator and its medical applications, *Designs* **3**, 2, 22.
4 Fang C., Tong T., Bu T., Cao Y., Xu S., Qi Y., Zhang C. (2020) Overview of power management for triboelectric nanogenerators, *Adv. Intell. Syst.* **2**, 2, 1900129.
5 Hu T., Wang H., Harmon W., Bamgboje D., Wang Z. (2022) Current progress on power management systems for triboelectric nanogenerators, *IEEE Trans. Power Electron.* **37**, 8, 9850–9864.

6 Venugopal K., Shanmugasundaram V. (2022) Effective modeling and numerical simulation of triboelectric nanogenerator for blood pressure measurement based on wrist pulse signal using comsol multiphysics software, *ACS Omega* **7**, 30, 26863–26870.
7 Bhatia D., Jo S.H., Ryu Y., Kim Y., Kim D.H., Park H.-S. (2021) Wearable triboelectric nanogenerator based exercise system for upper limb rehabilitation post neurological injuries, *Nano Energy* **80**, 105508.
8 Nazar A.M., Idala Egbe K.-J., Abdollahi A., Hariri-Ardebili M.A. (2021) Triboelectric nanogenerators for energy harvesting in ocean: a review on application and hybridization, *Energies* **14**, 18, 5600.
9 Tan D., Zeng Q., Wang X., Yuan S., Luo Y., Zhang X., Tan L., Hu C., Liu G. (2022) Anti-overturning fully symmetrical triboelectric nanogenerator based on an elliptic cylindrical structure for all-weather blue energy harvesting, *Nano-Micro Lett.* **14**, 1, 124.
10 Mariello M. (2022) Recent advances on hybrid piezo-triboelectric bio-nanogenerators: materials, architectures and circuitry, *Nano. Adv.* **2**, 1, 64–109.
11 Zi Y., Niu S., Wang J., Wen Z., Tang W., Wang Z.L. (2015) Standards and figure-of-merits for quantifying the performance of triboelectric nanogenerators, *Nat. Commun.* **6**, 1, 8376.
12 Vasandani P., Mao Z.-H., Jia W., Sun M. (2016) Design of simulation experiments to predict triboelectric generator output using structural parameters, *Simul. Model. Pract. Theory* **68**, 95–107.
13 Adly M.A., Arafa M.H., Hegazi H.A. (2021) Modeling and optimization of an inertial triboelectric motion sensor, *Nano Energy* **85**, 105952.
14 Cheng G., Lin Z.H., Lin L., Du Z.L., Wang Z.L. (2013) Pulsed nanogenerator with huge instantaneous output power density, *ACS Nano* **7**, 8, 7383–7391.
15 Li X., Xu G., Xia X., Fu J., Huang L., Zi Y. (2019) Standardization of triboelectric nanogenerators: progress and perspectives, *Nano Energy* **56**, 40–55.
16 Xia X., Fu J., Zi Y. (2019) A universal standardized method for output capability assessment of nanogenerators, *Nat. Commun.* **10**, 1, 4428.
17 Meng Z., Chen L. (2020) Theoretical maximum efficiency and higher power output in triboelectric nanogenerators, *Energy Rep.* **6**, 2463–2475.
18 Chen X., Han C., Wen Z., Liu Y. (2022) Theoretical boundary and optimization methodology of contact-separation triboelectric nanogenerator, *Appl. Mater. Today* **29**, 101685.

## Appendix A

### Calculation of the conversion efficiency

The differential equation which governs the evolution of the charge $Q$ carried by the mobile electrode is derived. Figure 1 shows that the voltage at the capacitor terminals is:

$$U = -E_{\mathrm{a}} \times z - E_{\mathrm{d}} \times h_{\mathrm{d}}. \tag{A1}$$

The electric field in the air gap is:

$$E_{\mathrm{a}} = \frac{-Q}{A_{\mathrm{d}}\varepsilon_0}. \tag{A2}$$

In the dielectric, the electric induction is:

$$D_{\mathrm{d}} = \frac{Q_0}{A_{\mathrm{d}}} - \frac{Q}{A_{\mathrm{d}}}, \tag{A3}$$

where $Q_0 = \sigma A_{\mathrm{d}}$. So, the electric field within the dielectric is:

$$E_{\mathrm{d}} = -\frac{Q - Q_0}{A_{\mathrm{d}}\varepsilon_0\varepsilon_r}. \tag{A4}$$

Finally, the voltage at TENG terminals is:

$$U = -\frac{\sigma h_{\mathrm{d}}}{\varepsilon_0\varepsilon_r} + \frac{1}{A_{\mathrm{d}}\varepsilon_0}\left(z + \frac{h_{\mathrm{d}}}{\varepsilon_r}\right)Q. \tag{A5}$$

As $U = -R\,\mathrm{d}Q/\mathrm{d}t$, the differential equation for the charge $Q$ is:

$$R\frac{\mathrm{d}Q}{\mathrm{d}t} = \frac{\sigma h_{\mathrm{d}}}{\varepsilon_0\varepsilon_r} - \frac{1}{A_{\mathrm{d}}\varepsilon_0}\left(z + \frac{h_{\mathrm{d}}}{\varepsilon_r}\right)Q. \tag{A6}$$

The efficiency of the triboelectric generator expressed in terms of the voltage $U$ and charge $Q$ is (see Sect. 2.1):

$$\eta = \frac{-\oint U\mathrm{d}Q}{\frac{1}{2} \times U_{\max} Q_0}. \tag{A7}$$

We define the dimensionless voltage $u = U/U_{\max}$ and charge $q = Q/Q_0$.

Then the efficiency expressed in terms of the dimensionless variables is:

$$\eta = -2\oint u\mathrm{d}q. \tag{A8}$$

From equation (A5), we calculate the reduced voltage:

$$u = qz - \beta(1 - q). \tag{A9}$$

As $\oint \beta(1-q)\mathrm{d}q = 0$ (over a cycle $\oint \mathrm{qdq} = 0$ and $\oint \mathrm{dq} = 0$), the efficiency can be expressed by:

$$\eta = -2\oint qz\mathrm{d}q. \tag{A10}$$

So, the knowledge of $q(t)$ over a period is sufficient to calculate the efficiency of a CS-TENG.

Another expression for efficiency is derived. Efficiency can be written in the form: $\eta = -\oint \mathrm{zdq}^2$. The function $g = zq^2$ is a state function. So $dg = q^2\mathrm{dz} + \mathrm{zdq}^2$ and $\oint dg = 0$. Then $-\oint \mathrm{zdq}^2 = \oint \mathrm{q}^2\mathrm{dz}$ and finally, one can write efficiency as follows:

$$\eta = \oint q^2\mathrm{d}z. \tag{A11}$$

The last expression can be related to the work done by the electrostatic force during a cycle. This force is proportional to $q^2$.The following equality:

$$\oint \frac{q^2}{2}\mathrm{d}z = -\oint u\mathrm{d}q \tag{A12}$$

expresses the law of conservation of energy over a period. The left expression is proportional to the mechanical work done over a cycle (input) by the external force counterbalancing the electrostatic force. The right expression is proportional to the electrical energy transferred to the load over a cycle (output).